Thermal Imaging for Discharge and Velocity Measurements in Open Channels

E. Jackson[1], D. Admiraal[2], D. Alexander[3], J. Stansbury[4],
J. Guo[5], D. Rundquist[6], and M. Drain[7]

[1]Dept. of Electrical Engineering, University of Nebraska – Lincoln, 209N WSEC Lincoln, NE 68588-0511; email: ethanj007@gmail.com

[2]Dept. of Civil Engineering, University of Nebraska – Lincoln, W348 Nebraska Hall, Lincoln, NE 68588-0531; email: dadmiraal@unl.edu

[3]Dept. of Electrical Engineering, University of Nebraska – Lincoln, 209N WSEC Lincoln, NE 68588-0511; email: dalexander1@unl.edu

[4]Department of Civil Engineering, University of Nebraska – Lincoln, 1110 S 67th St., PKI 205C, Omaha, NE 68182-0178; email: jstansbury@mail.unomaha.edu

[5]Department of Civil Engineering, University of Nebraska – Lincoln, 1110 S 67th St., PKI 204D, Omaha, NE 68182-0178; email: junkeguo@unlnotes.unl.edu

[6]School of Natural Resources, University of Nebraska – Lincoln, 307 Hardin Hall Lincoln, Nebraska 68588-0973; email: drundquist1@unl.edu

[7]The Central Nebraska Public Power and Irrigation District; 415 Lincoln St, PO Box 740, Holdrege, NE 68949-0740; email: mdrain@cnppid.com

Abstract
Thermal imaging cameras are powerful tools for measuring the temperature distributions on the surfaces of water bodies. The velocity distribution of a water surface can also be determined by recording the motion of the water surface temperature distribution with a thermal imaging camera and then applying particle image velocimetry (PIV) methods to sequential thermal images to obtain the velocity distribution. In this paper we discuss field and laboratory measurements of velocity distributions in open channel flows using a thermal imaging camera. The laboratory measurements are relatively simple comparisons of measured and calculated velocities for flows in a 71-*cm* wide channel with actively heated water surfaces. The field measurements include measurements of water velocity in a large power canal from an oblique camera angle with variations in image resolution. The oblique images are rectified and analyzed to determine velocities in the canal. The surveying and rectification processes are described in the paper, and resulting velocity

measurements are presented. None of the field measurements of velocity distributions utilize active heating of the water surface.

Introduction

Recently, significant advances in infrared cameras have made them extremely sensitive temperature measurement devices. Several researchers have begun measuring water surface flow phenomena with such cameras. For example, Jähne and Haußecker (1998) demonstrated the use of thermal imagery for investigating exchange of gases at the air-water interface, Jessup and Phadnis (2005) investigated geometric properties and velocities associated with microscale breaking waves using thermal imaging cameras, and Zhang and Harrison (2004) used infrared imaging techniques to observe temperature and velocity distributions of a wind driven water surface.

Infrared cameras can be used to track the velocities of thermal structures in a wide array of natural and artificial flows using Infrared Particle Image Velocimetry (IR-PIV), an appealing technique for two reasons. First, the "seed particles" can be patches of water with temperatures that differ slightly from those of the main flow, and apart from small density and viscosity effects, the velocities of coherent temperature patches will be equivalent to the velocity of the remainder of the water surface. Second, in many situations, there are natural or existing temperature gradients that are detectable with sensitive thermal cameras, eliminating the need for artificially seeding the flow with patches of warm water.

In this paper, the use of thermal cameras for measuring velocities and discharges in free surface flows will be explored in two settings, a 71-*cm* wide laboratory channel with hot water used to seed the flow, and a 20-*m* wide canal for which thermal images of the flow were gathered at oblique angles, filtered, rectified, and analyzed. In both cases, resulting velocity measurements are promising. As the sensitivity and accuracy of thermal cameras improves, the technique investigated in this paper is likely to play a significant role in analyzing flow fields.

Laboratory Experiments

Laboratory experiments were performed in the 0.71-*m* wide by 10-*m* long flume depicted in Figure 1. Water was supplied to the flume by the laboratory pump. The bed of the flume was nearly horizontal, and depth in the flume was controlled by adjusting the depth at the outlet using a weir. The test section was located 7.3 *m* downstream of the flume inlet tank. Two point gauges were used to measure depth on either side of the test section. The upstream point gauge was located 4.90 *m* upstream of the test section, and the downstream point gauge was located 1.93 *m* downstream of the test section. A hot water source was installed 3.76 *m* upstream of the control section. The hot water source was continuously cycled on and off every five seconds. The hot water sprayed from a diffuser onto a plastic gutter that allowed the water to trickle onto the surface without causing significant disturbance to the flow.

A FLIR Systems ThermaCAM S65HSV thermal imaging camera was installed at the test section directly above the water and was used to record the temperature of the water surface at 30 frames per second. The S65HSV has a spectral range of 7.5 to 13 μm and a thermal sensitivity of 50 mK at 30°C. Resolution of the camera is 320 pixels by 240 pixels and images can either be stored to a high-density flash card or can be transferred directly to a camera via an IEEE 1394 interface. The camera was installed inside a canvas tent to prevent reflections from laboratory lighting and other objects radiating heat from influencing the flow measurements.

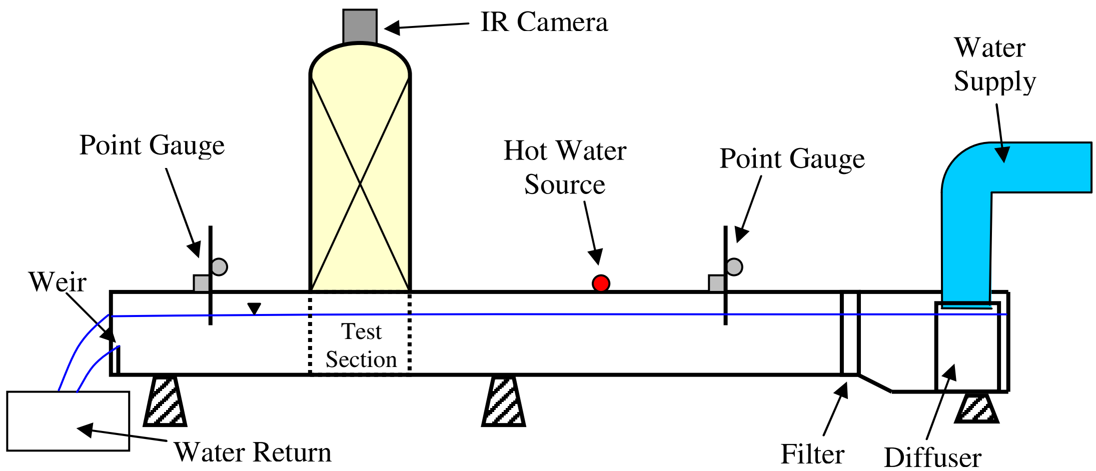

Figure 1 *Experimental flume layout*

Although multiple flow rates and seeding rates were tested in the flume, only the tests for one flow rate and one seeding rate are reported in this paper for the sake of brevity. Results from the flume experiments are given in Table 1. The flow rate to the flume was measured with a V-notch weir and was maintained at between 12 and 13 *L/s* for the tests shown in Table 1. Five weir heights were installed at the end of the flume, and the resulting water depths in the flume are recorded in the table.

Table 1 *Flume experiments*

Test	*Supply Discharge (L/s)*	*Weir Height (cm)*	*Upstream Depth (cm)*	*Downstream Depth (cm)*	*Average Depth (cm)*	*Average Seeding Rate (L/s)*	*Seed Water Temp. (°C)*	*Flume Water Temp. (°C)*
1	12.7	5.1	7.29	8.53	7.91	0.0209	42.6	20.8
2	13.1	8.9	10.32	11.74	11.03	0.0204	44.1	20.7
3	12.2	16.5	18.81	20.16	19.49	0.0214	44.7	20.9
4	12.5	23.5	25.88	27.27	26.58	0.0203	42.8	20.3
5	12.3	29.2	30.90	32.24	31.57	0.0215	43.7	20.6

The seeding rate for the tests in Table 1 is approximately 1/600 of the total flow rate. It was found that for tests with lower flow (~3 *L/s*) with high depths the hot water tended to spread in the flow direction, making it more difficult to measure streamwise velocity. For high flows (> 30 *L/s*) with low depths, the seed water mixed rapidly with the flume water, reducing signal-to-noise ratio. However, for the tests shown in Table 1, seed water mixed slowly in both the streamwise and transverse directions, creating thermal patterns like those shown in Figure 2.

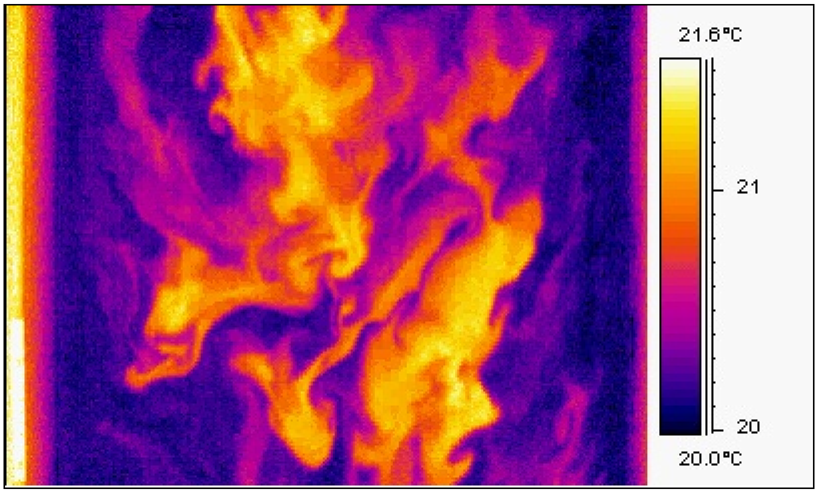

Figure 2 *Example thermal image of a flow seeded with hot water*

Sequences of images gathered with the infrared camera were converted into individual files that store the temperature distribution as an array. The arrays were imported into a particle image velocimetry program and were used to determine velocity distributions. For each weir height in Table 1, ten pairs of images were filtered using a 9 pixel median filter to reduce background noise and were interrogated using a minimum quadratic difference (MQD) formulation (Gui and Merzkirch, 2000). Other methods of correlation (e.g., Fast Fourier Transforms) were attempted but of those tried, the MQD formulation performed best. The MQD formulation was applied to a 5 by 4 array of 64 x 64 pixel interrogation windows with a search radius of between 8 and 10 pixels, depending on the time separation between images and the estimated flow velocity. A total of 200 surface velocities were calculated for each of the five tests in Table 1.

The few vectors that were incorrect were either indeterminate because no correlation was found or biased towards zero because of low signal-to-noise ratio. Indeterminate vectors were not included in final calculations. Although it is plausible that a method of removing the low velocity vectors could be found, that was not carried out for the results presented in this paper.

The surface velocities calculated for each weir height were converted to average velocities for the water column by assuming that the power law was valid and that side wall effects were negligible. In this case, the average velocity is 7/8 of the surface velocity measured with the thermal camera. Average velocities were also calculated using the discharges and average depths given in Table 1. The average velocities computed from the surface temperature measurements are plotted against the average velocities measured using the V-notch weir and point gauges in Figure 3. Each average velocity measured with the thermal camera consists of 200 individual measurements, and we also calculated standard deviations of these velocities. The vertical error bands in Figure 3 show two standard deviations above and below ($\pm 2\sigma$) the mean PIV velocity. The horizontal error bands shown in the figure are estimates of uncertainty ($\pm 2\sigma$) of average velocities computed from weir and point gage measurements. Average velocities measured with the thermal camera are within about 10% of computed average velocities. Differences may be because the wide channel assumption and application of the power law may be incorrect in some cases, the flow is non-uniform, the signal-to-noise ratio of the camera images is not high enough, and the V-notch weir has some error associated with it. Nevertheless, the resulting velocity measurements are reasonably accurate.

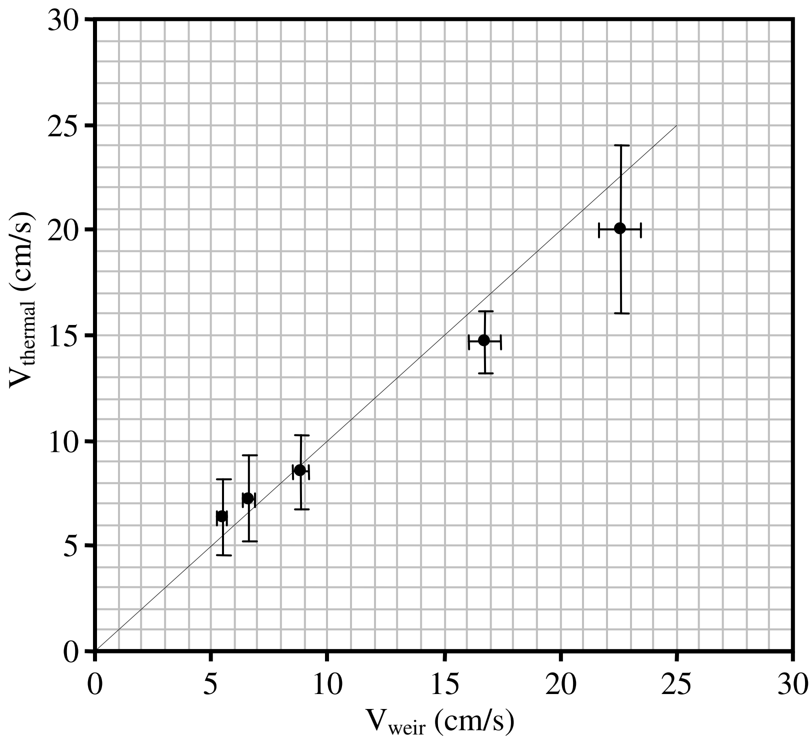

Figure 3 *Average velocity in the laboratory flume computed using thermal image velocimetry measurements versus average velocity computed from weir and stage measurements*

Field Measurements

Field measurements were carried out on Nebraska Public Power District's (NPPD) power canal at the outlet of Sutherland Reservoir in Sutherland, Nebraska. The thermal imaging camera was affixed to a surveying total station and the total station was set up on the north bank, overlooking the canal. Mounting the camera to the total station allowed us to survey the relative positions of five targets on the south side of the canal and three targets on the north side of the canal and to use the target positions to calibrate images gathered with the camera. The images collected with the camera were oblique, and had to be rectified. Before rectifying the images, the images were filtered with a nine pixel median filter to reduce background noise. The calibration targets were then converted to X and Y coordinates, corresponding x and y image coordinates were found in the thermal images for each target, and images were rectified following the method prescribed by Fujita et al. (1997, 1998).

A representative rectified thermal image is shown in Figure 4. The scale of the image is shown in the lower right hand corner of the image. The velocity distribution shown in the image was determined by applying the MQD formulation to five pairs of rectified images. Interrogation was performed on 128 by 128 pixel regions spaced at approximately 1 *m* along a transect of the channel. The resulting velocity vectors from the five pairs of images were averaged with corresponding vectors from the same location, and the resulting velocity distribution is overlain onto Figure 4.

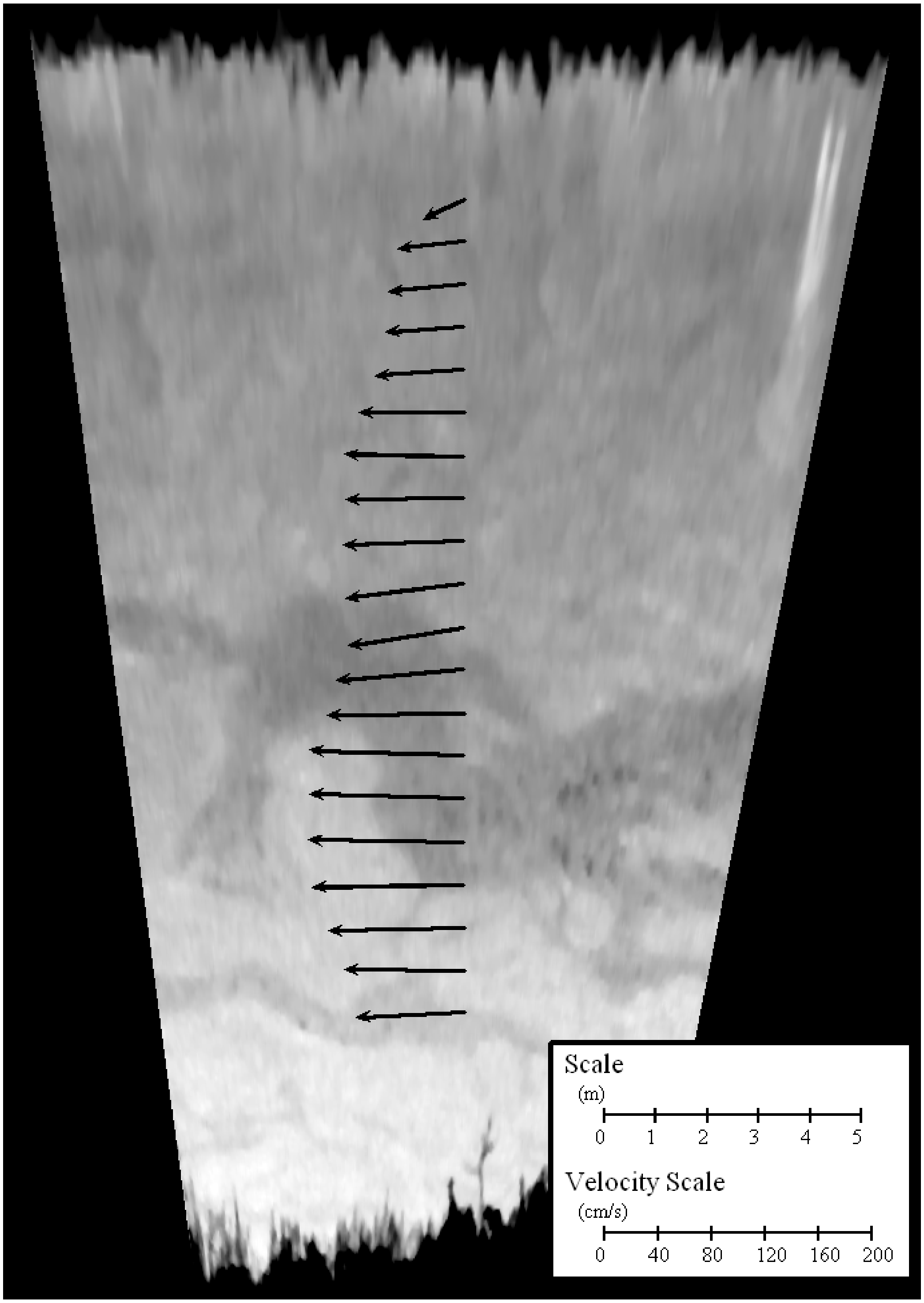

Figure 4 *Rectified thermal image and velocity distribution in the power canal for unseeded flows. Flow shown in the figure is from right to left*

The flow shown in Figure 4 was not seeded, but it should be noted that the flow comes from a reservoir not far upstream of the test site. Outflows from the reservoir may not be as isothermal as other flows of interest, though there is certainly not wide variation in surface temperature based on thermal camera measurements.

Unfortunately, the flowmeter that NPPD uses to measure flowrate immediately upstream of the site shown in Figure 4 was not working on the day that the thermal images were gathered. NPPD has provided discharge measurements for the canal at a downstream gauging location, but we do not yet have canal bathymetry for the test site. Once this information is provided, we will be able to directly verify the measurements shown in Figure 4. In our experience, riprap lined canals like this one typically have velocities on the order of 1 *m/s*, and the measurements shown in Figure 4 are certainly reasonable.

Conclusions

A thermal imaging camera was used in laboratory and field tests to measure water surface velocities. The surfaces of the laboratory flows were seeded with hot water, and resulting average velocities compared well with average velocities computed using a V-notch weir and average depth measurements. The device was also shown to be useful for measuring the surface velocity distribution in an unseeded canal in the field, though measured velocities were not yet verified at the time that this paper was submitted. Oblique images of the flow were filtered and rectified, and subsequent analysis of the resulting thermal images provided reasonable (though unverified) velocity distributions. In future work, the camera will be redeployed in field settings where the flow can be easily verified.

Acknowledgments

The authors express their gratitude to the Nebraska Center for Energy Sciences Research and the Nebraska Public Power District for providing funding for this research and assisting with field work.

References

Fujita, I., Aya, S., and Deguchi, T. (1997) “Surface velocity measurement of river flow using video images of an oblique angle,” *Proceedings XXVIIth IAHR Conference, Theme B, Vol. I*, San Francisco, CA, 227-232.

Fujita, I., Muste, M., and Kruger, A. (1998) “Large-scale particle image velocimetry for flow analysis in hydraulic engineering applications,” Journal of Hydraulic Research **36(3)**, 397-414.

Gui, L., and Merzkirch, W. (2000) “A comparative study of the MQD method and several correlation-based PIV evaluation algorithms,” *Experiments in Fluids*, **28**, 36-44.

Jähne, B. and Haußecker, H. (1998) “Air-water gas exchange,” *Annual Review of Fluid Mechanics*, **30**, 443-468.

Jessup A.T. and Phadnis, K R (2005) "Measurement of the geometric and kinematic properties of microscale breaking waves from infrared imagery using a PIV algorithm," *Measurement Science and Technology*, **16**, 1961-1969.

Zhang, X and Harrison, S. (2004) "A laboratory observation of the surface temperature and velocity distributions on a wavy and windy air–water interface," *Physics of Fluids*, **16(1)**, L5-L8.